Macroscopic measure of the cohesive length scale: Fracture of notched single-crystal silicon

Nicholas P. Bailey* and James P. Sethna
Department of Physics, Cornell University, Ithaca, New York 14853, USA
(Received 19 December 2002; revised manuscript received 30 May 2003; published 13 November 2003)

We study atomistically the fracture of single-crystal silicon at atomically sharp notches with opening angles of 0° (a crack), 70.53°, 90° and 125.3°. Such notches occur in silicon that has been formed by etching into microelectromechanical structures and tend to be the initiation sites for failure by fracture of these structures. Analogous to the stress intensity factor of traditional linear elastic fracture mechanics which characterizes the stress state in the limiting case of a crack, there exists a similar parameter K for the case of the notch. In the case of silicon, a brittle material, this characterization appears to be particularly valid. We use three interatomic potentials; that which gives critical K values closest to experiment is the modified embedded atom method (MEAM). Because the units of K depend on the notch angle, the shape of the K versus angle plot depends on the units used. In particular when an atomic length unit is used the plot is almost flat, showing—in principle, from macroscopic observations alone—the association of an atomic length scale to the fracture process. Moreover the normal stress on the actual fracture plane at this distance from the notch tip turns out to be even flatter and emerges as a possible fracture criterion, namely 33 MPa at a distance of one Å (for MEAM silicon).

DOI: 10.1103/PhysRevB.68.205204 PACS number(s): 81.05.Cy, 81.40.Np, 83.60.−a

I. INTRODUCTION

This paper presents computational work on the atomistic mechanisms of fracture. Fracture is a difficult problem in general because it is inherently multiscale. We have identified a geometry—the so-called notch geometry—which is suitable for atomistic calculations of fracture processes for the following three reasons. (1) Unlike simulations involving cracks, there is no need to introduce ''seed'' cracks, since there is already an opening—and hence a singular stress field when any load is applied. (2) There is reason to believe that the experimental specimens are atomically sharp and thus that there is a good correspondence at the atomic level between the experimental and simulated systems. (3) The dependence of the experimental critical stress intensity on notch angle allows one to infer an atomic length scale even before any atomistic calculations have been done. Apart from understanding fracture processes, this system is a useful test of interatomic potentials; the variation in observed behavior with interatomic potential is one of the themes of this paper.

There has been recent experimental[1–3] and theoretical[4] interest in fracture in sharply notched single-crystal silicon samples. Such samples have technological importance because silicon is a commonly used material in the fabrication of MEMS devices; the etching process used tends to create atomically sharp corners due to highly anisotropic etching rates.[3] Failure in such devices is often a result of fracture which initiated at sharp corners.[5] In the case of a notch, there exists a parameter K analogous to the stress intensity factor of traditional fracture mechanics, which parametrizes the elastic fields in the vicinity of the notch. Suwito *et al.*[2,3] have carried out a series of experiments which have (i) established the validity of the stress intensity factor as a fracture criterion in notched specimens and (ii) measured the critical stress intensities for several notch geometries. On the theoretical side Zhang[4] has carried out an analysis which models the separation of cleavage planes by a simple cohesive law, and thereby derived a formula for the critical stress intensity as a function of notch opening angle. The material properties which enter this formula are the elastic constants and the parameters of the cohesive law, the peak stress $\hat{\sigma}$, and the work of separation Γ_0. This recent activity has prompted us to investigate the phenomenon of fracture in notched silicon using atomistic simulations. In this paper we present direct measurements of the critical stress intensity for different geometries (i.e., notch opening angles) and compare them to the experimental results of Suwito *et al*. We apply a load by specifying a pure K field of a given strength (stress intensity factor) on the boundary of the system. In doing this we are effectively using the result of Suwito *et al*. that the notch stress intensity factor is indeed the quantity which determines fracture initiation, so we can ignore higher order terms in the local stress field.

Elastic fields near a notch. The essential geometry of a notch is shown in Fig. 1. The notch opening angle is denoted γ and the half angle within the material, which is the polar angle describing the top flank, is β (thus $\beta=\pi-\gamma/2$). As discussed in detail by Suwito *et al.*,[2,3] it is fairly straightforward to solve the equations of anisotropic linear elasticity for a notched specimen. The formalism used is known as the Stroh formalism,[6] which is useful for dealing with materials with arbitrary anisotropy in arbitrary orientations, as long as none of the fields depend on the z coordinate (this will be the out-of-plane coordinate; note that this does not restrict the

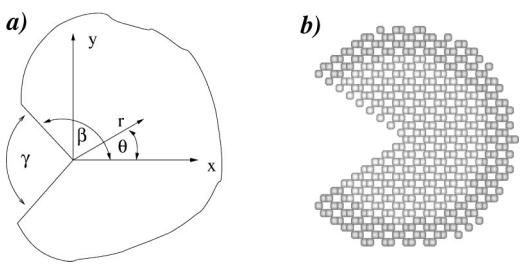

FIG. 1. (a) Notch schematic and notation and (b) silicon crystal with a notch; the darker layer is fixed boundary atoms.

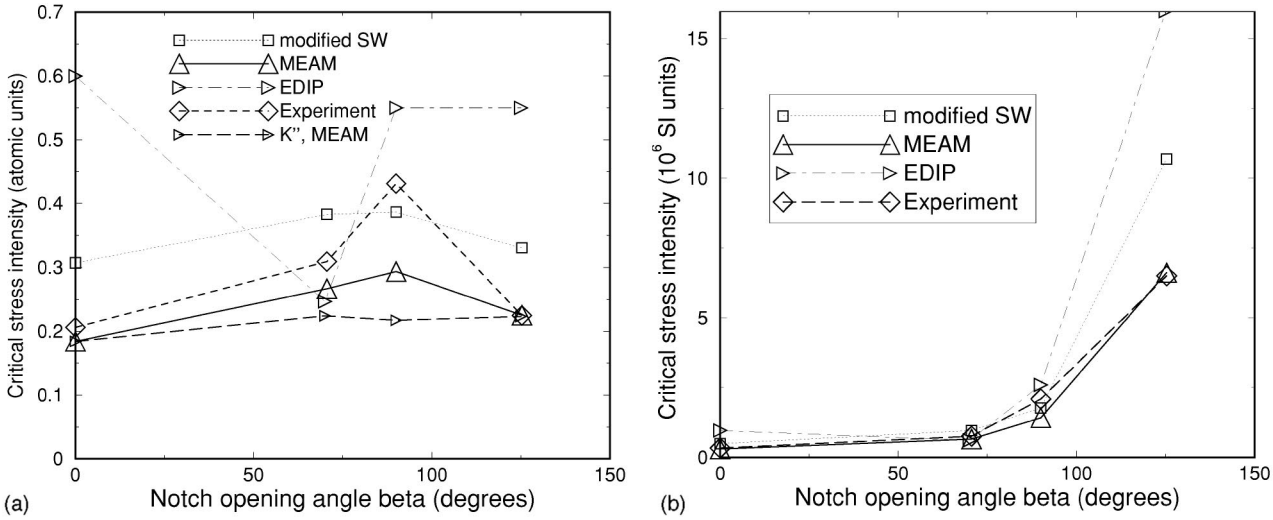

FIG. 2. Critical stress intensity K versus notch opening angle γ. (a) Units based on eV and Å and (b) SI units. The unusual, fractional units of length in the critical stress intensity make the shapes of these curves dependent on the choice of length units. In Sec. IV B and Fig. 7 we will discuss how the unit of length δ which makes the critical stress intensity nearly flat is a natural material-dependent length scale, perhaps a macroscopic manifestation of a kind of cohesive length. Also shown in (a) is the quantity K'' for the MEAM potential only (see text).

deformation itself to be in plane). Here we only consider mode I (symmetric) loading. The displacement and stress fields for a notch can be written as

$$u_i = K r^{\lambda} g_i(\theta), \tag{1}$$

$$\sigma_{ij} = K r^{\lambda - 1} f_{ij}(\theta), \tag{2}$$

where λ plays a role similar to an eigenvalue; its value is determined by applying the traction-free boundary conditions to the notch flanks. There is an infinity of possible values for λ of which we are interested in those in the range $0<\lambda<1$, which give rise to a singular stress field, often known as the K field, at the notch tip. This is entirely analogous to the singular field near a crack tip, which is simply the limiting case where γ goes to zero ($\beta \to \pi$), and λ becomes one half. Further details of the Stroh formalism, as applied to the notch geometry, are given in Appendix B. The complete elastic solution involves the whole infinity of values for λ, corresponding to different multipoles of the elastic field. Negative values of λ correspond to more singular fields which are associated with properties of the core region stemming from the nonlinear atomistic nature of this region; they do not couple to the far-field loading. $\lambda>1$ corresponds to fields which are less singular, and do not influence conditions near the notch tip, since the displacements and stress vanish there. They are, however, essential to represent the full elastic field throughout the body, and ensure that boundary loads and displacements (whatever they may be) are correctly taken into account. This is the basis for asserting that only the K field is important. This field is unique among the multipoles in that it both couples to the far-field loading and is singular at the notch tip. Thus the stress intensity factor must characterize conditions at the crack tip, and therefore a critical value K_c is associated with the initiation of fracture. The validity of this approach hinges on the validity of linear elasticity to well within the region in which the K field dominates.

Our main results are the plots of Fig. 2, which show the dependence of K_c on notch opening angle, in two different systems of units. The dependence of the shape on the units is very significant, as we will see. To understand this, first notice from Eq. (2) that the units of K and therefore K_c are stress/length$^{\lambda-1}$ which depends continuously on the notch angle γ through λ. Hence the shape of a plot of K_c against notch angle depends on the units used to make the plot. In metric/SI units K_c changes by an order of magnitude between 70° and 125° whereas if an atomic scale unit of length is used the plot is nearly flat [Figs. 2(b) and 2(a), respectively]. The significance of this fact will be discussed further below.

II. SIMULATIONS

A. Geometry

We simulated a cylindrical piece of silicon with a notch, making a shape as in Fig. 1(b), consisting of an inner core region and an outer boundary region. By focusing on just the initiation of fracture we avoid the need for large systems since we are not interested in the path the crack takes after the fracture (if we were, we would have a problem when the crack reached the edge of the core region and hit the boundary which is only a few lattice spacings away). We consider three notch geometries, which we call the 70° (actually 70.529°), 90°, and 125° (actually 125.264°) geometries, respectively, referring to the notch opening angles. The 70° sample has {111} surfaces on the notch flanks and the plane of the sample is a {110} surface. The 90° sample has {110} surfaces on the flanks and the plane is a {100} surface (in this case the crystal axes coincide with the coordinate axes). The

125° sample has a {111} on the bottom flank and a {100} surface on the top flank, while the plane of the sample is a {110} plane. In addition, we studied the zero degree notch geometry, corresponding to a standard crack. The crack plane is a {111} surface and is the *xz* plane in the simulation, and the direction of growth is the ⟨211⟩ direction, which is the *x* direction in the simulation. The radius of the inner, core region in almost all the cases presented is 5 lattice spacings or about 27 Å. The exceptions were the crack geometry for the EDIP potential (core radius was 7.5 lattice spacings—the ductile behavior of the potential necessitated a larger size) and the 90° geometry with the MEAM potential (core radius was four lattice spacings because this potential is computationally more demanding). The coordinate system in each case is oriented so that the plane of the sample is the *xy* plane and the notch is bisected by the *xz* plane.

B. Potentials

The question of the reliability of interatomic potentials continues to plague researchers, particularly in the context of simulations of brittle fracture (for a review of potentials used for brittle fracture of silicon see Holland and Marder[7]). The purpose of this work is not to claim that a particular potential is superior to others, but to investigate a particular geometry with atomistic simulations. To avoid limitations that might be associated with a particular potential, we have used three different silicon potentials. The first is a modified form of the Stillinger-Weber[8] potential (mSW), in which the coefficient of the three body term has been multiplied by a factor of 2. This has been noted by Hauch *et al.*[9] to make the SW potential brittle; they were unable to obtain brittle fracture with the unmodified SW potential. However it worsens the similarity to real silicon in other respects such as melting point and elastic constants.[9–11] The second potential is a more recent silicon potential known as the environment-dependent interatomic potential (EDIP),[12,13] which is similar in form to SW but has an environmental dependence that makes it a many-body potential. Bernstein and co-workers[14–16] have used EDIP to simulate fracture in silicon. They reported a fracture toughness about a factor of 4 too large when compared with experiment, and that fracture proceeds in a very ductile manner, accompanied by significant plastic deformation and disorder. A reason for the failure of empirical potentials proposed in Ref. 16 is that their short-ranged nature necessarily requires large stresses to separate bonds. This possibly explains the differences found with our third potential, the modified embedded atom method (MEAM) of Baskes.[17] This is a many-body potential similar to the embedded atom method but with angular terms in the electron density; it has been fit to many elements including metals and semiconductors. A significant feature of this potential is its use of ''three-body screening'' in addition to the usual pair cutoff distance. This means that atoms in the bulk see only their nearest neighbors, while surface atoms, on the other hand, can see any atoms above the surface (for example, on the other side of a crack) within the pair cutoff distance. The pair cutoff has been set to 6 Å to allow the crack surfaces to see each other[18] even after they have separated. The MEAM potential has been used successfully to simulate dynamic fracture in silicon,[19] and we have found it to be the most reliable potential in our studies of notch fracture.

C. Boundary conditions

The boundary conditions are as follows: in the *z* direction (out of the page) there are periodic boundary conditions. The thickness of the sample in this direction is always one or two repeat distances of the lattice in that direction. For the 70° and 125° geometries the repeat distance is $\sqrt{2}a$, where a is the cubic lattice constant; for the 90° geometry it is $2a$. In the plane, the boundary conditions are that a layer of atoms on the outside of the system has the positions given by the analytic formula (1) for displacements from anisotropic linear elasticity, with a specified stress intensity factor K. The thickness of the layer is twice the cutoff distance of the potential, in order that the core atoms feel properly surrounded by material.[26] We interpret the displacement formulas in terms of Eulerian coordinates, using an iterative procedure to compute the current positions. The numbers of core atoms were 890, 894, 1260, and 892, for the 0° (crack), 70°, 90°, and 125° systems, respectively (except for the EDIP/crack case where the core radius was 7.5 lattice constants; there the number of core atoms was 2002). The number of boundary atoms depends on the potential (through the cutoff distance); it is typically about 500 atoms. For the most part no special consideration was given to the lattice origin, which meant that by default it coincided with the notch tip.[27] In a few cases it was necessary to shift the position of the origin in order to make sure that the notch flanks were made cleanly, in particular so that the {111} flanks in the 70° and 125° geometries were complete close packed {111} surfaces, rather than having dangling atoms.

D. Critical stress intensities

The simulation consists of alternating the following two steps. (1) We increment the value of K by a small amount, changing the positions of the boundary atoms accordingly. (2) We relax the interior atoms as follows. First we run about 50 steps of Langevin molecular dynamics with a temperature of 500–600 K; the purpose of this is to break any symmetry (the 70° and 90° samples are symmetric about the *xz* plane). It is still a zero temperature simulation; these finite temperature steps are simply a way to introduce some noise. Next we run 500 time steps of the dynamical minimization technique known as ''MDmin'' (a Verlet time step is carried out, but after each velocity update, atoms whose velocities have negative dot products with their forces have their velocities set to zero). Finally 500 time steps of conjugate gradient minimization are carried out. We observe that the combination of both types of minimization is more effective (converges to a zero force state more quickly) than either alone. The procedure generally results in the atoms having forces of around 10^{-5} eV/Å.

The initial value for K could be zero, however, it turns out to be possible to start from a fairly large value of K by applying the analytic displacements to the whole system at

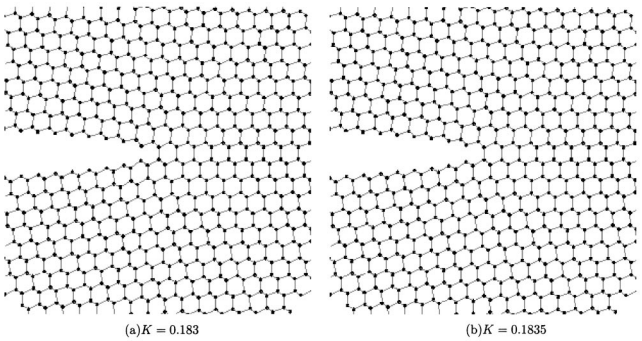

FIG. 3. Crack geometry, before and after crack growth, MEAM potential.

first. When the critical K value K_c is not yet known the increment size is chosen reasonably large to quickly find the K_c. When this has been found, the simulation is restarted from a value below the critical value with smaller increments and a more accurate value for K_c found. The increment is a measure of the uncertainty in K_c.

III. RESULTS

A. Observed fracture behavior

We observe brittle cleavage of the simulated crystals at definite values of K for all geometries using the mSW and MEAM potentials, but only for the 70° geometry when using the EDIP potential. Figures 3 and 4 show snapshots of the system just after fracture initiation process for the different geometries with the MEAM potential (in Fig. 3, which is the case of a crack, the process is strictly growth rather than initiation, and the configuration immediately before the crack extended is also shown for comparison). We also show in Figs. 5 and 6 the corresponding snapshots for the mSW and EDIP potentials, respectively, in the 90° geometry; here we observe three different behaviors for three different potentials—providing a cautionary demonstration of the limitations of empirical potentials.

In the 70° system [Fig. 4(a)] fracture occurs along a {111} plane. There are two choices for this, symmetrically placed with respect to the *xz* plane. Here all three potentials produced brittle behavior; this was the only geometry in which the EDIP potential did so. Possible reasons for this exception are discussed in Sec. IV. However, this behavior is quite sensitive to the initial configuration: when the origin was not shifted as mentioned in Sec. II D, so that the notch flanks had dangling atoms, the EDIP behavior was quite different: the notch blunted to a width of several atomic spacings.

In the 90° geometry the easy cleavage planes are the {110} planes which are extensions of the notch flanks. The MEAM potential behaves in the manner most consistent with experiment, namely, cleaving on {110} planes, and switching from one to the other—this is illustrated dramatically in Fig. 4(b). Experimentally, switching between planes, when it happens, occurs over longer length scales (25 μm for the 70° case[2]), although the behavior at atomic length scales has not been examined. Too much should not be read into the switching we observe, because once cleavage has occurred over such distances the proximity of the boundary probably has a large effect on the effective driving force on the crack.

For the 125° geometry [Fig. 4(c)], there are again two {111} planes to choose from but they are not symmetrically placed. Fracture occurs for the mSW and MEAM potentials on the one closest to the *xz* plane, i.e., closest to the plane of maximum normal stress, which is the $(11\bar{1})$ plane. The direction of growth is $[2\bar{1}\bar{1}]$, and growth proceeds much more readily than in the other notch geometries, presumably because it is almost along the maximum stress plane. A more complete presentation of the fracture behavior for the different geometries and potentials can be found in an earlier version of this manuscript (Ref. 20).

B. Critical stress intensities

The values of K_c, for the different potentials as well as from experiment, are listed in Table I and plotted in Fig. 2. The increment size for K is listed as an estimate of the error in K_c. The values for ductile fracture from the EDIP potential are marked with an asterisk as an indication that the definition of K_c in these cases is problematic. The experimental value for the crack geometry is from Ref. 21. Notice that the critical stress intensities for different angles are almost the same in atomic units, and differ by more than a factor of 10 in standard units.[28] To check for finite size effects, we repeated the measurement on the 70° geometry, but with larger radius of 8 Å, using the MEAM potential. In this case K_c was determined to be 0.262 ± 0.001, or about 1.7%

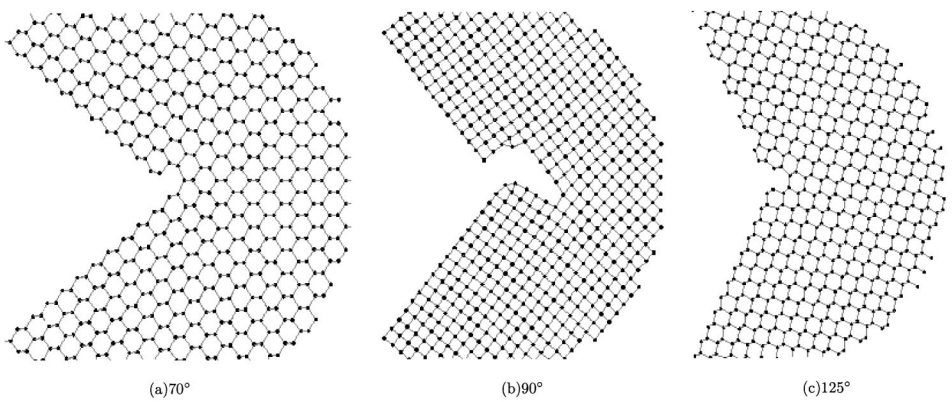

FIG. 4. Snapshots after fracture initiation in notched geometries with the MEAM potential.

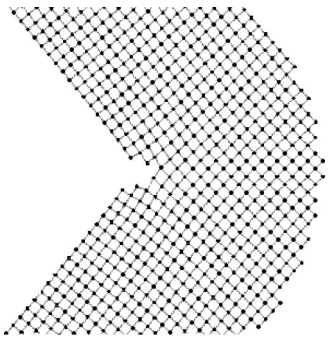

90° geometry, mSW potential, $K = 0.3871$.

FIG. 5. 90° geometry, mSW potential, $K=0.3871$.

lower than the value from the smaller system. This indicates that finite size effects are small, but not negligible. To compensate for them without using larger systems a flexible boundary method could be used, involving higher order ''multipoles'' of the elastic field, appropriate for the notch (i.e., solutions with $\lambda<0$), which could be relaxed.

For the crack cases we can make a comparison of our results with the so-called Griffith criterion for crack propagation. This comes from setting the energy release rate equal to twice the surface energy. An expression for the mode I energy release rate in terms of the stress intensity factor is given in Ref. 22; setting it equal to twice the surface energy leads to the following expression for the critical stress intensity factor:

$$\mathbf{K}_{\text{Griffith}}=\left(\frac{2\gamma}{\pi b_{22}\text{Im}[(\mu_1+\mu_2)/(\mu_1\mu_2)]}\right)^{1/2}, \qquad (3)$$

where μ_1 and μ_2 are the roots of a characteristic polynomial which depends on the elastic constants and b_{22} is an element of the compliance tensor for plane strain. The ratio K_c/K_{Griffith} is associated with lattice trapping, when fracture is brittle. This ratio is 1.57 for the mSW potential and 1.12 for MEAM. These values are, respectively, somewhat larger and somewhat smaller than the ratio 1.25 determined by Pérez and Gumbsch using total energy pseudopotential calculations[23] (our K_c corresponds to their K_+). In the EDIP case, where fracture proceeds only accompanied by significant plastic deformation, K_c is four times the Griffith value.

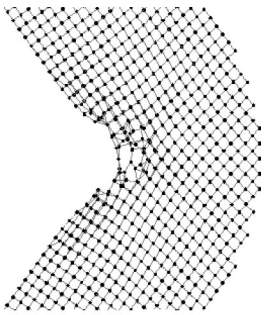

90° geometry, EDIP potential, $K = 0.6$.

FIG. 6. 90° geometry, EDIP potential, $K=0.6$.

TABLE I. Critical stress intensity values for different geometries and potentials, including experimental data from Refs. 2,3.

Potential	Geom.	K_c	Error	Griffith	K_c(SI)
mSW	0	0.3068	0.00036	0.1951	4.9×10^5
mSW	70	0.3832	0.00036		9.6×10^5
mSW	90	0.3863	0.00035		1.78×10^6
mSW	125	0.3304	0.00016		1.07×10^7
EDIP	0	0.6*	0.02	0.1463	9.6×10^5
EDIP	70	0.2465	0.001		6.1×10^5
EDIP	90	0.5–0.6*	0.0005		2.4–2.8×10^6
EDIP	125	0.5–0.6*	0.001		1.5–1.8×10^7
MEAM	0	0.184	0.0005	0.1641	3×10^5
MEAM	70	0.2665	0.0005		6.57×10^5
MEAM	90	0.2935	0.0005		1.42×10^6
MEAM	125	0.22	0.0005		6.47×10^6
Expt	0	0.2060		0.1776	3.3×10^5
Expt	70	0.31	10%		7.6×10^5
Expt	90	0.43	10%		2.1×10^6
Expt	125	0.22	10%		6.5×10^6

IV. DISCUSSION

A. Comparison of computed and experimental K_c

Comparisons between simulations and experiment are easiest when the data are plotted in atomic scale units whereby the apparent dependence on notch angle is much weaker: the data for the two brittle potentials make a gentle, almost horizontal, curve. The experimental data mostly lie between that for the MEAM potential and that for the mSW potential, but significantly closer to the former. The exception is the 90° case where the experimental value jumps to higher than the mSW value. Since the curves from the two potentials are very similar in shape—the main difference seems to be an overall shift or factor—and the jump in the experimental value at 90° is a departure from this shape, it would not be meaningful to assert that the mSW potential does a better job in predicting K_c in the 90° case. For the other angles the MEAM values are more or less within experimental error of experiment: the error (standard deviation across all the tested samples) is close to 10% in all cases (the error is not available for the crack case), and the percentage differences of the MEAM values with respect to the experimental values are -10, -14, -32, and $-0.5\,\%$ for the 0°, 70°, 90°, and 125° geometries, respectively. The 0.5% is clearly fortuitous. Note that the experimental error bar is not enough to account for the anomalously high value for the 90° case; there must be some feature of the physics or energetics of fracture initiation in this geometry that is missing from the others, and missing from the simulation.

It should be noted that part of the difference between the mSW and MEAM values can be ascribed to the difference in surface energies of these two potentials. For the {111} surface, mSW predicts an 18% larger surface energy than MEAM (23% for the {110} surface). If we assume that the square root dependence of K_c on γ_s given by the Griffith criterion remains valid for arbitrary notch angles then we

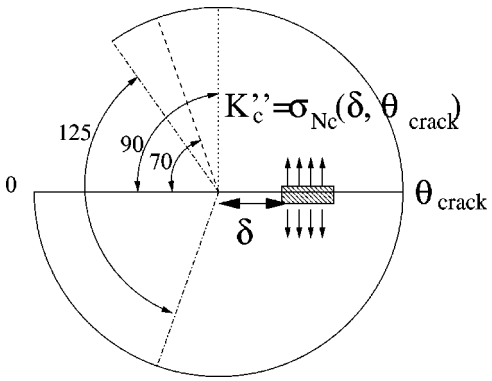

FIG. 7. Illustration of physical significance of the length scale δ and the quantity K_c''.

would expect K_c values roughly 10% larger than the MEAM ones. However, the difference ranges between 30 and 65 % so differences in surface energies cannot alone account for the differences in K_c. The mSW potential is, of course, not meant as a quantitative potential for Si. The artificial doubling of the three-body term makes it brittle but spoils the SW fit to the properties of Si.

B. Emergence of cohesive length scale and fracture criterion

The most interesting feature of the unit dependence is that it seems to provide a direct link from macroscopic measurements to a microscopic length scale. From a continuum point of view, one incorporates atomistic effects into fracture via a cohesive zone, a region ahead of the crack tip where material cleaves according to a specified force-separation law. One of the parameters of such laws is the length scale—the distance two surfaces must separate before the attractive force goes to zero—which for a brittle material is an atomic length scale. It is this scale that one would identify from the plot of K_c versus angle. Note that one can only identify a scale, and not an actual length parameter, in particular because the different geometries that are involved in the plot involve different fracture surfaces, with presumably different force-separation parameters. A more intuitive way to see the emergence of this length is to note that the angle-dependent factor f_{22} for the 22 component of stress in Eq. (2) is unity for $\theta=0$. If we define a new stress intensity whose units are independent of notch geometry as $K=K'\delta^{1-\lambda}$ by introducing an explicit length parameter δ, it is clear from dimensional analysis that K' will be independent of angle when δ is chosen to correspond to the unit of length which makes the $K-\gamma$ plot flat. K' has a physical interpretation as the value of σ_{22} on the plane that bisects the notch, at a distance δ in front of the notch tip (see Fig. 7). From a critical stress intensity factor as a function of notch angle we have inferred something much more intuitive—independent of notch geometry, there is a critical normal stress associated with a particular distance ahead of the notch tip, this distance (for Si, and likely also for other brittle materials) being an atomic length scale, of order Å. As explained above, this is not an exact statement, since the curve is not exactly flat. We can in fact go further by taking knowledge of the actual fracture plane into account. Using the Stroh formalism we compute the angular factors needed to obtain the normal stress at the fracture plane for each geometry. For the MEAM potential these factors are 1, 0.839935, 0.739143, and 0.990571 for the 0°, 70°, 90°, and 125° geometries, respectively (they are almost the same for other potentials). Multiplying K' (or K measured in length units of δ) by these factors gives the normal (opening) stress on these planes at the distance δ, which we denote K''. The long-dashed curve in Fig. 2 shows K_c'' for the MEAM potential. It noticeably flatter than $K_c(K_c')$. This degree of flatness allows us to propose that the quantity K'' may in fact be used as a fracture criterion in these notched systems. The mean value of K_c'' for the MEAM potential is 0.21 eV/Å=33 MPa, thus the fracture criterion is simply that fracture is expected to occur when the normal stress at a distance of one Å from the notch or crack tip reaches 33 MPa. We wish to stress that even in the absence of knowledge of the fracture planes we can infer the length scale from K_c itself, showing that one is seeing here the signature of microscale physics imprinting itself on macroscopic measurements.

C. How closely do the model notches match experiments?

In our simulations, for a given potential, only one fracture behavior is observed, in contrast to what was observed in the experiments of Suwito *et al.*[2] Specifically, in the case of the 70° geometry, they observed three different ''modes'' (not to be confused with loading modes), including propagation on the (110) plane, yet we have observed cleavage only on {111} planes in this geometry. It is possible that finite temperature, and the relative heights of different lattice trapping barriers, play an important role here. More likely it is related to experimental microcracks or defects near the crack tip. In any case, it would be of great benefit to systematically calculate the barriers for different processes that can occur at a notch (or crack) tip, as a function of applied load. It should be noted that in comparing simulations involving such very small length scales (27 Å) to experiment it is appropriate to consider the question of whether the experimental notches are indeed as sharp as we have made our simulated notches. Suwito *et al.*[2] could only put an upper limit of 0.8 μm on the radius of curvature of their notches, although notch radii of the order of 10 nm have been reported in etched silicon.[3] The addition of just a few atoms right at the notch tip would presumably have a significant effect on the energetics of cleavage initiation. We have not made any investigation of this, and this question should be borne in mind given the absence of experimental data characterizing the notch tip at the atomic scale. Nevertheless, the success of our simulations provides an important indication that these notches are indeed atomistically sharp.

V. SUMMARY

We have determined by atomistic simulation the critical stress intensities to initiate fracture in notched single crystal silicon samples. The samples had angles of 0° (a crack), 70.5233°, 90°, and 125.264°—chosen so that the flanks of

the notches were low index crystal planes. These geometries correspond to those studied experimentally in measurements of critical stress intensities for fracture initiation. Of the three potentials used, modified Stillinger-Weber (mSW), environment-dependent interatomic potential (EDIP), and modified embedded atom method (MEAM), MEAM produced the most realistic behavior, which is consistent with simulations of dynamic fracture. The most interesting result of this paper is the near independence of K_c on notch angle when referred to an appropriate length scale. This is an atomic length scale, and we assert that it is the length scale associated with cohesive zones in continuum models of fracture. Furthermore, the value of the normal or opening stress on the observed fracture plane at this length scale is almost exactly flat and thus suggests a plausible fracture criterion for these systems (which include cracks): whether the opening stress at a characteristic distance attains a critical value (33 MPa at 1 Å for MEAM Si). In all, the notch system offers excellent opportunities for well controlled investigations of fracture with direct connection to experiment, including the use of a variety of atomistic simulation techniques going beyond those discussed in this paper (for example, the systematic calculation of energy barriers for cleavage and dislocation nucleation as a function of crack/slip system, etc).

ACKNOWLEDGMENTS

We thank Zhiliang Zhang for inspiration and helpful discussions, and Noam Bernstein for helpful discussions. We also thank Mike Baskes for help in coding the MEAM potential. This work was financed by NSF-KDI Grant No. 9873214 and NSF-ITR Grant No. ACI-0085969. Atomic position visualization figures were produced using the DAN program, developed by N. Bernstein at Harvard University and the Naval Research Laboratory.

APPENDIX A: UNITS AND CONVERSIONS

Three different sets of units are used in this paper. To each atomic potential (Stillinger-Weber, EDIP, MEAM) is associated a set of atomic units (EDIP and MEAM use the same units); also we often wish to use SI units to compare to experiment. In the context of this paper there is the further subtlety that the units of the chief quantity under consideration, namely, the stress intensity factor K, are not simple powers of base units but involve a nontrivial exponent λ which is a function of geometry and potential. In fact the SI units for K are $\mathrm{Pa\,m}^{1-\lambda}$ which for brevity we simply refer to as ''standard units'' in the paper.

The units for an atomic potential are determined by specifying the unit of energy and that of length (for dynamics the unit of time is determined from these and the particle mass). The SW potential as originally written down did not have units built into it. By taking the energy unit to be $\epsilon = 2.1672$ eV $= 3.4723\times10^{-19}$ J and the length unit to be $\sigma = 2.0951$ Å, the authors modeled molten silicon.[8] However other authors[24] have taken the energy unit to be $\epsilon = 2.315$ eV. The difference is not really important since we have modified the potential itself to make it more brittle so the resemblance to real silicon is reduced noticeably. When expressing quantities in terms of eV–Å units we use the second scaling which is more common. The EDIP and MEAM potentials have $\epsilon = 1$ eV and $\sigma = 1$ Å built in as their units. Since $\sigma \sim K r^{\lambda-1}$, the units of K are $[\text{stress}]/[\text{length}]^{\lambda-1} = [\text{energy}]/[\text{length}]^{2+\lambda}$, so to convert a value for K in atomic units to SI units, one uses the conversion factor $\epsilon/\sigma^{2+\lambda}$. Table II gives the factors for the three potentials and the geometries studied in this paper.

TABLE II. Unit conversion factors for K.

Potential	Geometry	λ	Factor
mSW	0	0.5	1602000
mSW	70	0.51954	2510000
mSW	90	0.54597	4620000
mSW	125	0.63047	32320000
EDIP	0	0.5	1602000
EDIP	70	0.51922	2490000
EDIP	90	0.54708	4730000
EDIP	125	0.62844	30840000
MEAM	0	0.5	1602000
MEAM	70	0.51875	2467000
MEAM	90	0.54794	4832000
MEAM	125	0.62639	29420000

APPENDIX B: STROH FORMALISM FOR NOTCHES

Here we summarize the application of the Stroh formalism to the notch problem. More details are available in Refs. 2,3,25. We can write the solution for the displacement field $\mathbf{u}$ and the stress function ϕ as

$$\mathbf{u} = \sum_{\alpha=1}^{6} \mathbf{a}_\alpha f_\alpha(z_\alpha), \tag{B1}$$

$$\phi = \sum_{\alpha=1}^{6} \mathbf{b}_\alpha f_\alpha(z_\alpha). \tag{B2}$$

The independent variable here is the complex variable $z_\alpha = x_1 + p_\alpha x_2$. The stress function ϕ determines the stresses through $\sigma_{i1} = -\phi_{i,2}$ and $\sigma_{i2} = \phi_{i,1}$. The p_α, $\mathbf{a}_\alpha$, and $\mathbf{b}_\alpha$ come from solving the following eigenvalue problem:

$$[\mathbf{Q} + p(\mathbf{R} + \mathbf{R}^{\mathbf{T}}) + p^2\mathbf{T}]\mathbf{a} = 0, \tag{B3}$$

where

$$\mathbf{Q} = \begin{bmatrix} C_{11} & C_{16} & C_{15} \\ C_{16} & C_{66} & C_{56} \\ C_{15} & C_{56} & C_{55} \end{bmatrix}, \quad \mathbf{R} = \begin{bmatrix} C_{16} & C_{12} & C_{14} \\ C_{66} & C_{26} & C_{46} \\ C_{56} & C_{25} & C_{45} \end{bmatrix},$$

$$\mathbf{T} = \begin{bmatrix} C_{66} & C_{26} & C_{46} \\ C_{26} & C_{22} & C_{24} \\ C_{46} & C_{24} & C_{44} \end{bmatrix}. \tag{B4}$$

The above is general within the context of two-dimensional anisotropic elasticity. To specify the notch problem we choose a form of the arbitrary function f to which we can apply the boundary conditions of the problem—that notch flanks are traction-free. The following choice does the trick:

$$f_\alpha(z_\alpha) = \frac{1}{\lambda} \frac{z_\alpha^\lambda}{\xi_\alpha(-\beta)^\lambda} \mathbf{b}^{\mathbf{T}}{}_\alpha \mathbf{q} = \frac{1}{\lambda} r^\lambda \left[\frac{\xi_\alpha(\theta)}{\xi_\alpha(-\beta)} \right]^\lambda \mathbf{b}^{\mathbf{T}}{}_\alpha \mathbf{q}, \tag{B5}$$

where $\xi(\theta) = \cos(\theta) + p_\alpha \sin(\theta)$ and $\mathbf{q}$ is to be determined. The traction with respect to a radial plane at angle θ is given by

$$\mathbf{t} = r^{\lambda-1} \sum_{\alpha=1}^{6} \left[\frac{\xi_\alpha(\theta)}{\xi_\alpha(-\beta)} \right]^\lambda \mathbf{b}_\alpha \mathbf{b}^{\mathbf{T}}{}_\alpha \mathbf{q} = \frac{\lambda}{r} \phi. \tag{B6}$$

With the above form the traction condition is already satisfied on the bottom flank $\theta = -\beta$. Applying the condition on the top flank leads to a matrix equation

$$\mathbf{K}(\lambda)\mathbf{q}(\lambda) = 0. \tag{B7}$$

The appropriate value of λ is determined by setting the determinant of the matrix equal to zero and solving the resulting equation numerically. In the range $0 < \lambda < 1$, two values can be found, corresponding to modes I and II, λ^{I} and λ^{II}. For a given λ, the vector $\mathbf{q}$ is determined up to a normalization which is related to how one defines the stress intensity factor K. Thus we obtain expressions for the displacements which are used in the simulation to place the boundary atoms. In the crack case, because λ^{I} and λ^{II} are degenerate at the value 1/2, the definition of modes I and II is a little subtle. The {111} plane is not a plane of symmetry of the cube, and thus one cannot expect to separate modes by their symmetry properties as in for example, the isotropic case; following Ref. 22, mode I is defined as that for which $\sigma_{12}(\theta = 0) = 0$ and mode II that for which $\sigma_{22}(\theta = 0) = 0$.

For the purpose of the simulations described in this paper, we calculated the Stroh parameters as follows. For each potential, the elastic constants were determined by standard methods (straining the supercell, relaxing, measuring the relaxed energy per unit undeformed volume and fitting to a parabola). This gives C_{11}, C_{12}, and C_{44}, which are the three independent constants for a cubic crystal. In the formulas for the displacements and stresses given above, the coordinate system is aligned with the notch (in that the negative x axis bisects the notch itself) and not with the crystal axes. So we must transform the elastic constants accordingly. Once we have the transformed constants we can construct the Stroh matrices **Q**, **R**, and **T**, and compute the Stroh eigenvalues and eigenvectors as above.

*Electronic address: nbailey@fysik.dtu.dk

[1] M.L. Dunn, W. Suwito, S.J. Cunningham, and C.W. May, Int. J. Fract. **84**, 367 (1997).

[2] W. Suwito, M.L. Dunn, and S.J. Cunningham, J. Appl. Phys. **83**, 3574 (1998).

[3] W. Suwito, M.L. Dunn, S.J. Cunningham, and D.T. Read, J. Appl. Phys. **85**, 3519 (1999).

[4] Z. Zhang (unpublished).

[5] W. Suwito, M. L. Dunn, and S. J. Cunningham (unpublished).

[6] T.C.T. Ting, *Anisotropic Elasticity: Theory and Applications* (Oxford University Press, New York, 1996).

[7] D. Holland and M. Marder, Adv. Mater. (Weinheim, Ger.) **11**, 793 (1999).

[8] F.H. Stillinger and T.A. Weber, Phys. Rev. B **31**, 5262 (1985).

[9] J.A. Hauch, D. Holland, M.P. Marder, and H.L. Swinney, Phys. Rev. Lett. **82**, 3823 (1999).

[10] D. Holland and M. Marder, Phys. Rev. Lett. **80**, 746 (1998).

[11] D. Holland and M. Marder, Phys. Rev. Lett. **81**, 4029 (1999).

[12] M.Z. Bazant, E. Kaxiras, and J.F. Justo, Phys. Rev. B **56**, 8542 (1997).

[13] J.F. Justo, M.Z. Bazant, E. Kaxiras, V.V. Bulatov, and S. Yip, Phys. Rev. B **58**, 2539 (1998).

[14] N. Bernstein *et al.* (unpublished).

[15] F.F. Abraham, N. Bernstein, J.Q. Broughton, and D. Hess, MRS Bull. **25**, 27 (2000).

[16] N. Bernstein and D. Hess, MRS Symp. Proc. No. 653 (Materials Research Society, Warrendale, PA, 2001), p. Z2.7.1.

[17] M.I. Baskes, Phys. Rev. B **46**, 2727 (1992).

[18] M. I. Baskes (private communication).

[19] C.P. Chen and M.H. Leipold, Phys. Rev. Lett. **89**, 085503 (2002).

[20] N.P. Bailey and J.P. Sethna, cond-mat/0301076, version 1 (unpublished).

[21] C.P. Chen and M.H. Leipold, Am. Ceram. Soc. Bull. **59**, 469 (1980).

[22] G.C. Sih, P.C. Paris, and G.R. Irwin, Int. J. Fract. Mech. **1**, 189 (1965).

[23] R. Pérez and P. Gumbsch, Phys. Rev. Lett. **84**, 5347 (2000).

[24] H. Balamane, T. Halicioglu, and W.A. Tiller, Phys. Rev. B **46**, 2250 (1992).

[25] P.E.W. Labossiere and M.L. Dunn, Eng. Fract. Mech. **61**, 635 (1998).

[26] It has to be twice because of the three- and many-body terms in the potentials.

[27] When applying singular elastic deformations, a check ensures that an atom sitting at the location of the singularity is simply not displaced.

[28] Note that the exact conversion factor depends on the eigenvalue λ which depends on the potential (see Appendix A), but for a given angle the dependence on potential is quite small.